JOURNAL OF NANO- AND ELECTRONIC PHYSICS
Vol. **9** No 3, 03007(4pp) (2017)

ЖУРНАЛ НАНО- ТА ЕЛЕКТРОННОЇ ФІЗИКИ
Том **9** № 3, 03007(4cc) (2017)

Investigating the Band Alignment of Zn(O, S) with Kesterite (Cu_2ZnSnS_4) Material for Photovoltaic Application

Margi Jani[1,*], Dhyey Raval[1,†], Abhijit Ray[1,‡]

[1] *Solar Research and Development Center & School of Solar Energy, Pandit Deendayal Petroleum University, Gandhinagar – 382007 India*

(Received 23 November 2016; revised manuscript received 10 May 2017; published online 30 June 2017)

This paper reports theoretical simulation of the band alignment of zinc oxysulfide Zn(O,S) with kesterite (Cu_2ZnSnS_4) material for the photovoltaic application. Zinc oxysulfide Zn(O,S) is selected for this study due to the possibility of band gap tailoring and non-toxicity. It is widely explored as a buffer layer for the fabrication of CZTS thin film solar cells. A detailed study is presented in order to investigate the consequences of band bending due to the use of Zn(O,S) as a buffer layer in Cu_2ZnSnS_4 (CZTS) solar cells and corresponding electrical performance is explored using one-dimensional simulation tool SCAPS. Presented analysis shows that the band-gap can be optimized through sulfur content variation, which is beneficial to reduce the band offset with the heterojunction partner material (i.e. CZTS). The optimization is done by monitoring the electrical performance of CZTS solar cells. The open circuit voltage (V_{oc}), short-circuit current density (J_{sc}), fill factor (FF) and efficiency (η) are found to vary in the range of 414 to 417 mV, 26.3 to 26.9 mA/cm^2, 21 % to 26 % and 2.3 to 2.8 % respectively with respect to variation in sulfur content in the range of 0 to 30 %.

Keywords: Zinc oxy-sulfide, Band alignment, Kesterite, CZTS, Photovoltaic.

DOI: 10.21272/jnep.9(3).03007 PACS numbers: 42.70.Nq, 72.40. + w

1. INTRODUCTION

Thin film solar cells from earth abundant and non-toxic elements have significantly high potential to lead the future photovoltaic developments within next decade. Some of the important photovoltaic absorbers are Cu_2ZnSnS_4, Cu_2SnS_3 and SnS [1, 2]. Among these earth abundant options, Cu_2ZnSnS_4 bears certain qualities in terms of economic processability like Spray deposition [3, 4], sol-gel and spin coating [5,6], very high absorption coefficient [7] in the visible spectrum and intrinsic p-type conductivity [8]. These absorber materials being inherently p-type semiconductors need a different n-type buffer layer. One of the major concerns associated with most of these hetero-junction solar cells directly affecting their efficiency is the discontinuity of their conduction and valence band, known as conduction band offset (CBO) and valence band offsets (VBO), respectively [9]. Zn(O,S) as a buffer layer partner with SnS, CIGS, CIS absorber layer has been well studied. Generally, CZTS solar cell is used with CdS buffer layer. The cadmium is a toxic material, the development of Cd-free buffer layers became an interesting research area in the field of chalcogenide solar cells. Different types of the buffer layers are explored for chalcogenide based thin film solar cells. Zinc based buffer layer like Zn(O,S), $Zn_{1-x}Sn_xO_y$ and $Zn_{1-x}Cd_xS$ are found to be promising alternative candidate for the purpose of the buffer layer to compete with CdS [10 – 12]. CIGS with Zn(O,S) buffer layer with a photovoltaic conversion efficiency of 16.4 % has been already reported [13]. From the literature survey, it is evident that the CZTS/Zn(O,S) is not well-explored compared to CIGS based solar cells. This article addresses the optimization of sulfur content in context with the discontinuity of their conduction and valence band.

The band diagram in a standard Cu_2ZnSnS_4/CdS heterojunction solar cell having an i-ZnO window layer and an Al-doped ZnO transparent conducting oxide (TCO) layer consists of a positive CBO. A positive CBO at the junction acts as a barrier to the photo-generated electrons moving from absorber layer towards n-type buffer layer, leading to a reduction in the open circuit voltage due to enhanced recombination [14]. Eventually, by moving the junction away from the physical interface, the interface recombination can be reduced [15, 16]. For a negative CBO, the junction moves towards the physical interface and hence the probability of recombination increases [17]. So, it is desirable for a heterojunction solar cell to bear a small but positive CBO [18].

The simulation is done for realistic device performance parameters using the software Solar Cells Capacitance Simulator in one dimension (SCAPS-1D). This software is helpful for finding the steady-state band diagram, recombination profile, carrier transport in 1-dimension based on the Poisson equation and the electron and hole continuity equations [19]. This paper reports theoretical simulation of the band alignment of zinc oxysulfide Zn(O,S) with kesterite (Cu_2ZnSnS_4) material for the photovoltaic application.

2. DEVICE AND BAND STRUCTURE DESCRIPTION

2.1 Device Structure

A typical CZTS thin film solar cell structure consists

* margi.jphd13@sse.pdpu.ac.in
† dhyey.rphd13@sse.pdpu.ac.in
‡ abhijit.ray@sse.pdpu.ac.in

of a p-type wide-band-gap absorber layer which is deposited on the Molybdenum (Mo) coated back glass substrate and an n-type buffer/window layer. The buffer layer forms a junction with the absorber layer leading to the absorption of maximum amount of incoming light. The criteria for buffer layer are listed here as 1) minimal absorption loss, 2) low surface recombination and 3) low electrical resistance in driving out the generated carriers. To satisfy such desired criteria, the buffer layer should be as thin as possible and should have a wider band gap in comparison with the absorber layer.

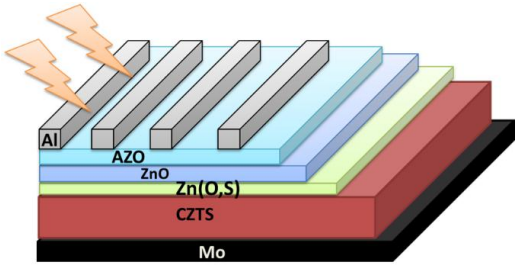

Fig. 1 – The device structure of CZTS/Zn(O,S) solar cell

Fig. 1 shows device structure of standard Cu_2ZnSnS_4 cell replacing CdS with non-toxic Zn(O,S) buffer layer. Simulation for Zn(O,S) buffer layer in CZTS solar cell has been done in this work. By varying sulfur concentration we can tune the bandgap for Zn(O,S). By selecting a suitable composition for Zn(O,S) system, optimum band offset was found.

2.2 Band Alignment with Cu_2ZnSnS_4 (CZTS)

The band alignment of Zn(O,S) with a standard Cu_2ZnSnS_4 absorber layer is shown in Fig. 1. In the band diagram of CZTS/Zn(O,S)/i-ZnO/AZO, the numbers represent the work function (Mo), electron affinity and the band-gap as per the layer position in the device with respect to the vacuum level.

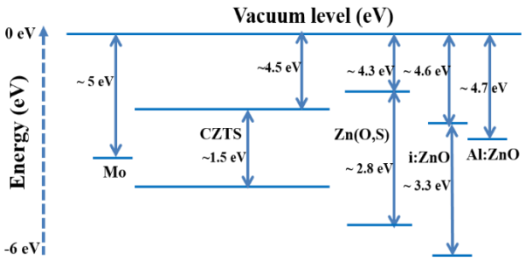

Fig. 2 – Band structure of CZTS with buffer material

The band diagram of CZTS solar cells is shown in Fig. 1 for a device thickness of 2.8 µm. The thickness of CZTS is taken to be 2 µm, beyond this, band bending starts due to the formation of heterojunction with Zn(O,S). A small shift observed at 2 µm represents the potential barrier formed due to positive shifting of CBO. The simulation shows that un-doped ZnS as a buffer layer forms barrier towards CZTS and impede the diffusion of electrons, whereas in the case of ZnO its conduction band minimum appears at a lower value than that of CZTS causing a large negative CBO, eventually the ZnO/CZTS interface recombination increases [20, 21]. It is clear that the band alignment is possible by adding sulfur in ZnO to form a solid solution, i.e. Zn(O,S). The various absorber layers such as SnS, $Cu(In,Ga)S_2$ and $CuInS_2$ already use Zn(O,S) buffer layer and the solar cell performance improves due to favorable CBO with the absorber layer [22]. To check the band bowing effect in the solid solution of Zn(O,S) with various possible economic chalcogenide absorbers (particularly CZTS), the software SCAPS-1D [23] has been used here.

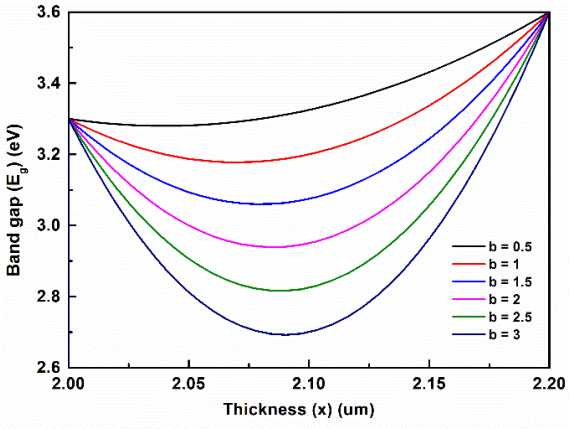

Fig. 3 – Band-bowing effect in solid solution of Zn (O,S)

As shown in Fig. 3 variation of band gap with S-concentration is estimated from ZnO (3.3 eV) to ZnS (3.6 eV) transition by parabolic nature of grading. It is observed that E_g is parabolically changing with increase in bowing parameter (b). Zn(O,S) corresponding to $b = 2.5$ has been used for estimating the performance of device and it is in accordance with Thankalekshmi and Rastogi [24]. Following equation has been used for calculating band gap values shown in Fig. 3 [25],

$$E_g(x) = x.E_g(ZnS) + (1-x).E_g(ZnO) - b(1-x).x \quad (2.1)$$

Where, b is bowing parameter and x shows Zn(O,S) position in the device due to graded sulfur profile.

3. SIMULATION PARAMETERS

The parameters used in the simulation are listed in Table 1. Parameters from the buffer layer, Zn(O,S): 1) band gap (E_g) (eV), 2) electron affinity (χ), 3) relative permittivity (ε_r), 4) carrier concentration (~N_D, the donor concentration assuming complete ionization at room temperature), 5) Mobility (μ), 6) Doping concentration (N_D) (1/cm^3), 7) Effective density of states in CB (1/cm^3) 8) Effective density of states in VB (1/cm^3) are the most important to determine diffusion current across the junction. Parameters required for the simulation are the effective density of states in the conduction and valence band, and the carriers' thermal velocity are constant at a fixed temperature is used from the literature [26 – 28].

4. RESULTS AND DISCUSSION

In CZTS/Zn(O,S) system, ZnO and ZnS should have no change of electron affinity with doping, because it only changes the electronic structure within the valence

Table 1 – Simulation parameters for device Structure [26 – 28]

Parameters for simulation	CZTS	Zn(O,S) (Buffer) S-variation	i-ZnO	Al:ZnO
Thickness (μm)	2.0	0.05	0.05	0.2
Bandgap (eV)	1.5	2.8 – 3.6	3.3	3.3
χ(eV)	4.5	4.3 – 3.9	4.6	4.7
Permittivity	10	8.49 – 8.3	9	9
CB (1/cm^3)	2.2×10^{18}	2.2×10^{18} – 6.3×10^{18}	2.2×10^{18}	2.2×10^{18}
VB (1/cm^3)	1.8×10^{19}	1.8×10^{19} – 6.0×10^{19}	1.8×10^{19}	1.8×10^{19}
μ_e (cm^2 /Vs)	100	100 - 50	100	100
μ_h (cm^2 /Vs)	25	25 – 20	25	25
Doping concentration (1/cm^3)	1.0×10^{16}	1.0×10^{11} – 1.0×10^{13}	1.0×10^{5}	1.0×10^{18}
Electron thermal velocity (cm/s)	1.0×10^{7}	1.0×10^{7}	1.0×10^{7}	1.0×10^{7}
Hole thermal velocity (cm/s)	1.0×10^{7}	1.0×10^{7}	1.0×10^{7}	1.0×10^{7}

and conduction band. Hence values are assumed to be constant and selected from the literature [14, 29]. For example, χ and ε_r were assumed to be constant and equal to that of ZnO in the case of *S*-content ranging from 0 – 20 %. They are assumed to be constant and equal to that of ZnS in the case of *S*-content varies in the range from 40 – 100 %. On the other side, the dielectric permittivity of the layer depends on frequency and the wave vector, so does the polarization. Fig. 1 shows the linear band diagram of Zn(O,S) relative to that of CZTS layer used for device performance calculations. As shown in Fig. 4(A), CBO which is the difference of χ from the CZTS and Zn(O,S) remains slightly positive at 0.2 eV for S-content in the range of 0-20%.

The CBO becomes more positive (at 0.6 eV) for S-content in the range of 40 – 100 %. The VBO is determined by the sum of valence band difference (Ev, absorber – E_v, buffer) and amount of net band bending (E_{bb}) [14, 29]. Obviously, the VBO as shown in Fig. 4(A) is always negative. The value of Ebb in the case of CZTS/Zn(O,S) junction has been experimentally obtained by Yan et al. [30] as 0.03 eV. The VBO thus shows minimum and maximum values of – 1.1 eV and -1.57 eV for the *S*-content of 20 % and 0 %, respectively.

As seen from the Fig. 4(B) the open circuit voltage (V_{oc}), and short-circuit current density (J_{sc}) varies from 414 to 417 mV and 26.3 to 26.9 mA/cm^2 respectively for sulfur variation of 0 – 30 %. It is found that max V_{oc} is found in the range 15 – 20 % sulfur concentration is 416 mV and J_{sc} is 26.65 mA/cm^2. As seen from Fig. 4(C), fill factor (FF) and efficiency (η) are found to vary in the range of 21 % to 26 % and 2.3 to 2.8 % respectively with respect to variation in the sulfur content of 0 – 30 %. It is found that max FF is found in the range of 15 – 20 % sulfur concentration is 25 % and η is found to be 2.75 %.

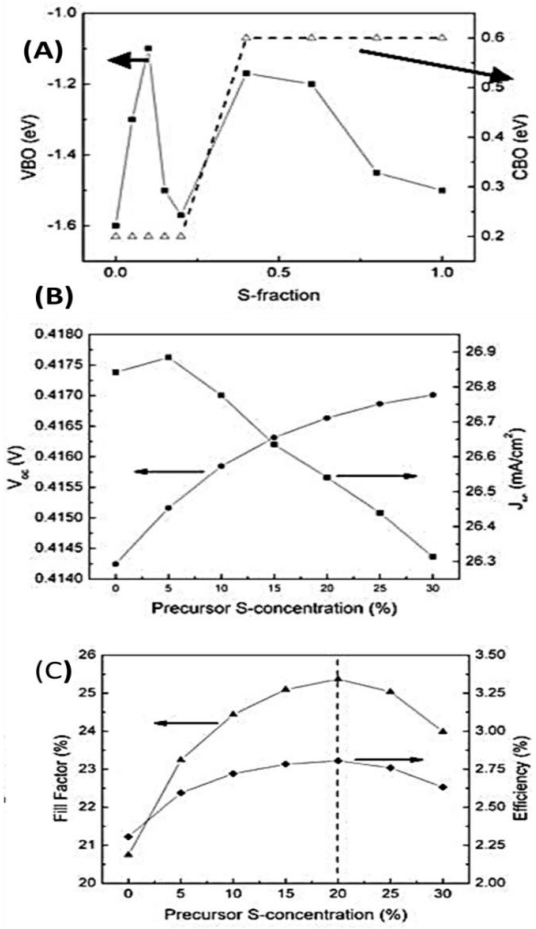

Fig. 4 – (A) The conduction and valence band offsets relative to CZTS and (B) & (C) the calculated output performance of the CZTS/Zn(O,S) heterojunction solar cell with variation in initial sulfur concentration in the doping range

5. CONCLUSIONS

The performance of a Cu_2ZnSnS_4 (CZTS) solar cell using Cd-free alternative buffer largely depends on the heterojunction band offset. Grading based band gap bowing effect in the Zn(O,S) system allows to select the composition content of sulfur at 20 %, so that the bowing parameter increased to 2.5 leading to an enhancement in the output performance by the improvement in the open-circuit voltage as confirmed by current-voltage analysis of a Zn(O,S)/CZTS heterojunction structure using SCAPS-1D.

ACKNOWLEDGEMENTS

Authors are grateful to the Dr. Brijesh Tripathi for scientific discussions.

REFERENCES

1. T.K. Todorov, J. Tang, S. Bag, O. Gunawan, T. Gokmen, Y. Zhu, and D.B. Mitzi, *Adv. Energ. Mater.* **3**, 34 (2013).
2. S. Bag, O. Gunawan, T. Gokmen, Y. Zhu, T. K. Todorov, and D. B. Mitzi, *Energy & Environmental Sci.* **5**, 7060 (2012).
3. Y.K. Kumar, G.S. Babu, P.U. Bhaskar, and V. S. Raja, *Sol. Energ. Mat. Sol. C* **93**, 1230 (2009).
4. M. Valdés, G. Santoro, and M. Vázquez, *J. Alloy. Compd.* **585**, 776 (2014).
5. P.K. Sarswat and M.L. Free, Phys. *Status Solidi A* **208**, 2861 (2011).
6. S. Kahraman, S. Çetinkaya, M. Podlogar, S. Bernik, H. Çetinkara, and H. Güder, *Ceram. Intern.* **39**, 9285 (2013).
7. S. Abermann, *Sol. Energ.* **94**, 37 (2013).
8. S. Delbos, *EPJ Photovol.* **3**, 35004 (2012).
9. A. Klein, *J. Phys.-Condens. Mat.* **27**, 134201 (2015).
10. C. Platzer-Björkman, C. Frisk, J. Larsen, T. Ericson, S.-Y. Li, J. Scragg, J. Keller, F. Larsson, and T. Törndahl, *Appl. Phys. Lett.* **107**, 243904 (2015).
11. R. Bhattacharya, K. Ramanathan, L. Gedvilas, and B. Keyes, *J. Phys. Chem. Sol.* **66**, 1862 (2005).
12. T. Nakada and M. Mizutani, *Jpn. J. Appl. Phys.* **41**, L165 (2002).
13. C. Platzer-Björkman, T. Törndahl, D. Abou-Ras, J. Malmström, J. Kessler, and L. Stolt, *J. Appl. Phys.* **100**, 044506 (2006).
14. A. Santoni, F. Biccari, C. Malerba, M. Valentini, R. Chierchia, and A. Mittiga, *J. Phys. D* **46**, 175101 (2013).
15. A. Niemegeers, M. Burgelman, and A. De Vos, *Appl. Phys. Lett.* **67**, 843 (1995).
16. R. Herberholz, V. Nadenau, U. Rühle, C. Köble, H. Schock, and B. Dimmler, *Sol. Energ. Mater. Sol. Cel.* **49**, 227 (1997).
17. Z.-Y. Dong, Y.-F. Li, B. Yao, Z.-H. Ding, G. Yang, R. Deng, X. Fang, Z.-P. Wei, and L. Liu, *J. Phys. D* **47**, 075304 (2014).
18. M. Bär, U. Bloeck, H.-J. Muffler, M. Lux-Steiner, C.-H. Fischer, M. Giersig, T. Niesen, and F. Karg, *J. Appl. Phys.* **97**, 014905 (2005).
19. P.-J. Lin, L.-Y. Lin, J.-L. Yu, S.-Y. Cheng, P.-M. Lu, and Q. Zheng, *J. Appl. Sci. Eng.* **17**, 383 (2014).
20. A. Okamoto, T. Minemoto, and H. Takakura, *Jpn. J. Appl. Phys.* **50** No 4s (2011).
21. T. Ericson, J.J. Scragg, A. Hultqvist, J.T. Wätjen, P. Szaniawski, T. Törndahl, and C. Platzer-Björkman, *IEEE J. Photovoltaics* **4**, 465 (2014).
22. S. Sharbati and J.R. Sites, *IEEE J. Photovoltaics* **4**, 697 (2014).
23. C. Adel, B.M. Fethi, and B. Brahim, *Int. J. Phys. Sci.* **9**, 250 (2014).
24. R.R. Thankalekshmi and A. Rastogi, *J. Appl. Phys.* **112**, 063708 (2012).
25. J. Van Vechten and T. Bergstresser, *Phys. Rev. B* **1**, 3351 (1970).
26. M. Patel and A. Ray, *Phys. B* **407**, 4391 (2012).
27. H. Ramli, S.K.A. Rahim, T.A. RAHIM, and M. M. Aminuddin, *Chalcogenide Letters* **10**, 189 (2013).
28. M. Olopade, O. Oyebola, and B. Adeleke, *Adv. Appl. Sci. Res.* **3**, 3396 (2012).
29. A. Klein, T. Löher, Y. Tomm, C. Pettenkofer, and W. Jaegermann, *Appl. Phys. Lett.* **70**, 1299 (1997).
30. C. Yan, F. Liu, N. Song, B.K. Ng, J. A. Stride, A. Tadich, and X. Hao, *Appl. Phys. Lett.* **104**, 173901 (2014).